Organic & Biomolecular Chemistry

Accepted Manuscript

Organic & Biomolecular Chemistry

Volume 15
Number 47
21 December 2017
Pages 9945-10124

rsc.li/obc

ISSN 1477-0520

ROYAL SOCIETY OF CHEMISTRY

PAPER
I. J. Dmochowski et al
Oligonucleotide modifications enhance probe stability for
single cell transcriptome in vivo analysis (TIVA)

ROYAL SOCIETY OF CHEMISTRY

rsc.li/obc

ARTICLE

Light-driven molecular pumps: entanglement of thermodynamic and kinetic effects in the photocontrolled threading-unthreading of pseudorotaxanes

Brian Sachini,[a,b] Chiara Taticchi,[a,b] Massimo Baroncini,[b,c] Stefano Corra[a,b] and Alberto Credi*[a,b]

Light-powered molecular pumps represent an intriguing class of artificial nanomachines capable of using the energy of photons to perform directional transport. Pseudorotaxanes composed of macrocyclic crown ethers that encircle axles based on azobenzene photoswitches and secondary ammonium recognition sites have emerged as promising architectures, as light can modulate both the kinetics and thermodynamics of complex formation, thereby enabling directionally biased motion by an energy ratchet mechanism. In this study, we examine the effect of photoisomerization on the threading-unthreading dynamics of a symmetrical axle bearing decoupled azobenzene and dibenzylammonium units. The results are compared with those obtained on a previously reported more compact axle in which the two units share a phenyl ring. We found that, while Z-azobenzene significantly slows down the (un)threading kinetics with respect to the E-isomer, it does not destabilize the pseudorotaxane. Hence, such a decoupling challenges a core design requirement for photoinduced molecular pumps – namely, the light-induced modulation of both energy barriers and binding affinities. Our results underscore the critical role of electronic and spatial proximity between the photoisomerizable unit and the ring recognition site in achieving coupled kinetic and thermodynamic control. These insights provide refined design principles for the development of efficient light-driven molecular pumps based on modular supramolecular motifs.

Introduction

The development of artificial molecular motors that can autonomously harness an energy source to move directionally under non-equilibrium conditions constitutes a grand challenge of modern nanotechnology.[1,2,3,4,5] Among these devices, molecular pumps – namely, systems in which a component translates unidirectionally with respect to another – are particularly interesting, both for the underlying fundamental concepts and the potential for applications in technology and medicine.[6,7,8]

Despite the abundance and relevance of biomolecular pumps in nature,[9] and the fact that a few outstanding examples of artificial molecular pumps powered by chemical,[10,11,12,13] electrical[14] or light[15,16,17] energy have been reported in the literature, the designed construction of this kind of devices remains extremely demanding, particularly if an autonomous behaviour (i.e. the ability to repeat the operation cycle when energy is provided under constant conditions) is desired.[18,19]

Among the different forms of energy to operate molecular pumps, light is particularly appealing because of the advantages offered by photoexcitation in terms of control, flexibility, reversibility and spatiotemporal resolution.[20,21,22]

We have previously described[15–17,23] an autonomous light-driven supramolecular pump based on a pseudorotaxane architecture, consisting (Figure 1a) of an oriented axle-type compound such as, for example, E-**1**H⁺, and a macrocycle such as dibenzo-24-crown-8-ether (**2**). The former contains (i) an azobenzene photoswitchable gate as a terminal unit, (ii) a secondary ammonium ion as the recognition site for the ring in the centre, and (iii) a non-photoactive "pseudo-stopper" at the other extremity.[24] The axle, being oriented, has a preferential threading-unthreading direction, which involves the azobenzene end when it is in the E-configuration (gate open), and the pseudo-stopper end when the azobenzene is in the Z-configuration (gate closed). Additionally, the complex of the ring with the E-axle is more stable than with the Z-axle. Therefore, after directional threading of the E-axle, photoirradiation triggers the E→Z isomerization and causes directional unthreading of a fraction of the complexes. Because light of the same wavelength can also induce the Z→E isomerization – both azobenzene configurations are photoreactive and exhibit absorption bands in the same spectral regions – autonomous operation can be achieved. Overall, light irradiation affords a periodic modulation of the non-symmetric energy landscape enabling an energy ratchet mechanism that rectifies the relative Brownian motion of the components (Figure 1b).[18,19]

[a.] Dipartimento di Chimica Industriale "Toso Montanari", Alma Mater Studiorum - Università di Bologna, Via Gobetti 85, 40129 Bologna, Italy.

[b.] Center for Light Activated Nanostructures (CLAN), Istituto ISOF-CNR, via Gobetti 101, 40129 Bologna, Italy.

[c.] Dipartimento di Scienze e Tecnologie Agro-Alimentari, Alma Mater Studiorum - Università di Bologna, Viale Fanin 40-50, 40127 Bologna, Italy.

ARTICLE

a

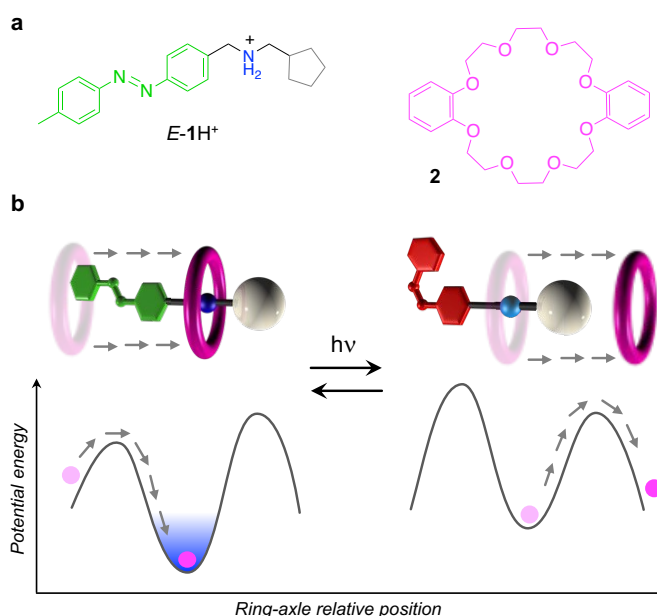
E-**1**H$^+$

2

b

Figure 1. (a) The molecular components of a pseudorotaxane-based photochemically driven molecular pump. (b) Cartoon representation of the photoinduced directional threading-unthreading movement and simplified potential energy diagram showing the light-dependent modulation of maxima and minima (ratcheting) at the basis of the pump mechanism.

A key aspect of the mechanism is that the photoisomerization of the azobenzene moiety affects both the thermodynamics (i.e. the stability of the complex, or the energy well) and the kinetics (i.e. the complexation rate, or the energy barrier) of threading-unthreading. Understanding the origin of these phenomena and their mutual influence is important for the development of novel supramolecular pumps based on similar blueprints.[25]

Previous experimental and computational investigations performed on a symmetric molecular axle containing two azobenzene terminal units (*EE*-**3**H$^+$, Figure 2)[26] suggested that the *EE* and *ZZ* isomers exhibit different slippage kinetics and stability as a result of a subtle combination of electronic and steric effects.[27] In this work, we aim at gaining more specific information on the role of the azobenzene photoswitch in the equilibria of pseudorotaxane formation. We synthesized a novel symmetric axle *EE*-**4**H$^+$ and compared its behaviour with that of *EE*-**3**H$^+$ (Figure 2). The former contains the same moieties of the latter, but in the new species the dibenzylammonium recognition site and the azobenzene units do not share a phenyl ring and are electronically decoupled owing to the presence of a short ethereal linkage. We envisioned that the spatial and electronic separation of these moieties could enable us to gain new insights into the consequences of photoswitching on the thermodynamic and kinetic parameters of threading-unthreading.
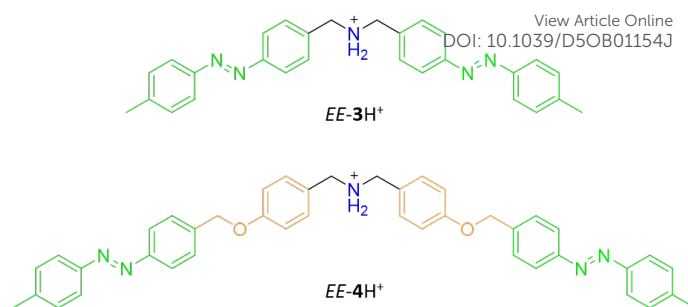
EE-**3**H$^+$

EE-**4**H$^+$

Figure 2. Structure formula of the symmetric axles *EE*-**3**H$^+$ and *EE*-**4**H$^+$.

Results and discussion

Dibenzo-24-crown-8-ether (**2**) is commercially available and *EE*-**3**H$^+$ was prepared according to the previously reported synthetic route.[26] The symmetric axle *EE*-**4**H$^+$ was synthesized in 8 steps starting from inexpensive starting materials with a convergent and scalable approach. The two intermediates **5** and *E*-**6**, whose synthesis is described in the Supporting Information, were connected via nucleophilic substitution. Subsequent Boc deprotection and salt exchange yielded the target species *EE*-**4**H$^+$ as hexafluorophosphate salt (Scheme 1). The compound was fully characterized by mass spectrometry, NMR and UV-visible spectroscopies (see the SI).

5   +   *E*-**6**

i) K$_2$CO$_3$, 18-crown-6, CH$_3$CN
ii) THF/HCl
iii) H$_2$O/NH$_4$PF$_6$

EE-**4**H$^+$

hv', Δ ⇅ hv
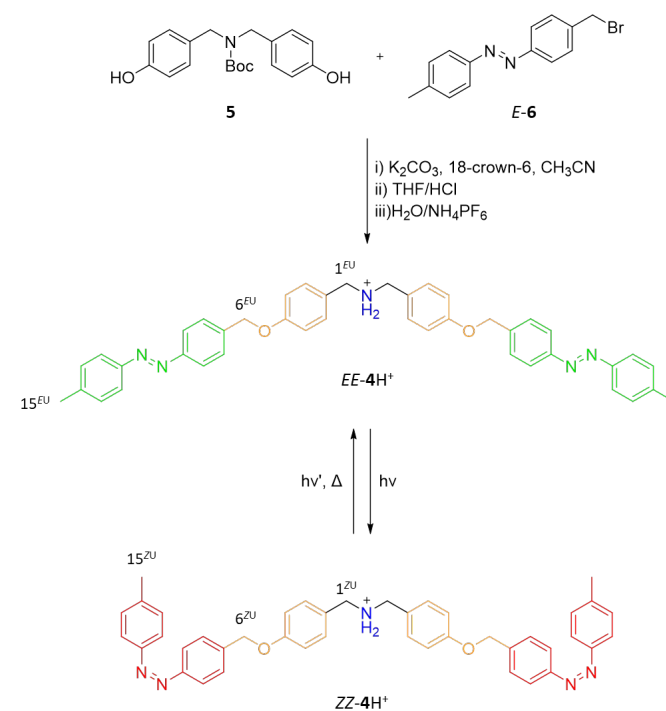
ZZ-**4**H$^+$

Scheme 1. Convergent synthetic pathway to *EE*-**4**H$^+$ and photoisomerization product *ZZ*-**4**H$^+$.

Regarding the photophysical and photochemical properties, in CH$_3$CN at room temperature, *EE*-**4**H$^+$ shows the typical absorption spectral features of azobenzene derivatives. Namely, an intense π-π* band (λ$_{max}$ = 329 nm) and a weaker and broader n-π* band (λ$_{max}$ = 441 nm), with molar absorption

coefficients twice those of E-**1**H^{+}. Irradiation with UV light (365 nm) causes the $E{\to}Z$ isomerization of the azobenzene units (Figure 3 and SI), while the $Z{\to}E$ transformation can be accomplished both photochemically, *i.e.* by irradiation with visible light (436 nm), or thermally. The value of the molar absorption coefficients, photoisomerization quantum yields, and the presence of clean isosbestic points throughout the irradiations, suggest that the two azobenzene units behave independently, in line with the observations on EE-**3**H^{+}.[26]
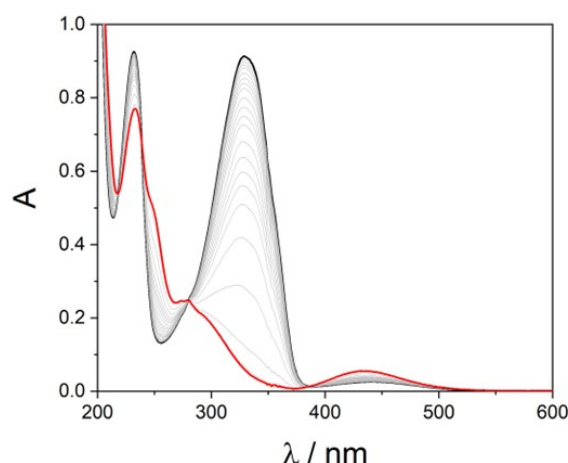

Figure 3. Absorption variations of a 1.6×10^{−5} M solution of EE-**4**H^{+} in CH₃CN (black line) upon irradiation at 365 nm until a photostationary state is reached (red line).

The ^{1}H NMR spectrum of EE-**4**H^{+} in CD₃CN exhibits two diagnostic resonances (Figure 4a): (i) the singlet associated with the methylene protons 1[EU] (4.15 ppm) and (ii) the resonance of the methylene protons 6[EU] (5.22 ppm). The photoisomerization of EE-**4**H^{+} was then investigated by irradiating the compound at 365 nm, a wavelength at which the ratio of the molar absorption coefficients of the E and Z azobenzene isomers is particularly high. Indeed, at the photostationary state (reached in about 25 minutes under our conditions, see the SI) a nearly quantitative (>98%) conversion to ZZ-**4**H^{+} is achieved, as estimated by the UV-Vis spectra and determined from the integration of diagnostic ^{1}H NMR signals (Figure 4d and experimental section).‡ As expected, for ZZ-**4**H^{+} a clear upfield shift of 6[ZU] methylene protons Conversely, those corresponding to methylene groups 1[ZU] remain unchanged. This result indicates that the central ammonium region in the new axle **4**H^{+} experiences a similar chemical environment in both the EE and ZZ isomers, in contrast with the behaviour of the previously reported axle **3**H^{+}.[26]

Upon mixing axle EE-**4**H^{+} and macrocycle **2**, resonances clearly indicating formation of complex EE-**4**H^{+}⊂**2** (Figure 4b).[26] In particular, the resonances of complex EE-**4**H^{+}⊂**2** associated with the methylene protons that are adjacent to the oxygen atoms (6[EC]) are shifted upfield (5.09 ppm; Figure 4b), and those associated with the methylene protons next to the ammonium center (1[EC]) are shifted downfield (4.56 ppm; Figure 4b).

Due to the low solubility of axle EE-**4**H^{+}, all NMR studies were performed in acetonitrile solutions whose concentration (about 2.0 mM) was accurately determined each time by employing an internal standard (see the SI). In these conditions, an association of the molecular components of about 30% was reproducibly observed in the presence of one equivalent of **2**, corresponding to a stability constant of the complex EE-**4**H^{+}⊂**2** (K_{EE}) of 330 M^{−1}. It is worth noting that the complex of **2** with EE-**4**H^{+} is significantly less stable than that with EE-**3**H^{+}, whose stability constant was found to be 820 M^{−1}, in line with previous data.[26] This observation is attributed to the electron rich nature of the methoxy spacer, which renders the ammonium centre of EE-**4**H^{+} a less efficient hydrogen bond donor than that of EE-**3**H^{+}. This observation is consistent with earlier studies on the complexation of dibenzylammonium guests by dibenzo-24-crown-8 ether (**2**).[28]
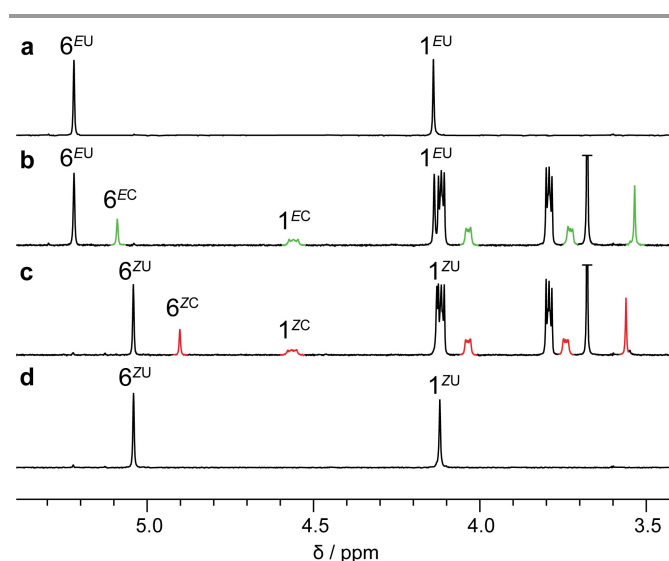

Figure 4. Stacked partial ^{1}H NMR (500 MHz, CD3CN, 298 K, 1.4 mM) spectra of (a) axle EE-**4**H^{+}, (b) a 1:1 mixture of EE-**4**H^{+} and crown ether **2**, (c) the same sample after exhaustive irradiation at 365 nm and (d) axle ZZ-**4**H^{+}.

The UV-vis spectroscopic characterization of the EE-**4**H^{+}⊂**2** and ZZ-**4**H^{+}⊂**2** complexes did not highlight remarkable differences with respect to that performed on the free axles and confirms the efficient photoisomerization of the azobenzene moieties. To structurally investigate the effect of light irradiation on the complex, a sample containing equimolar amounts of EE-**4**H^{+} and **2** was allowed to equilibrate in the dark to form the EE-complex and subsequently irradiated (λ_{irr} = 365 nm) to afford a photostationary state rich in ZZ-**4**H^{+}⊂**2**. The ^{1}H NMR spectra show that the resonances of the methylene protons (6) adjacent to the oxygen atom are distinguishable for all complexed (Figure 4: EE-**4**H^{+}⊂**2**, 5.03 ppm, 6[EC]; ZZ-**4**H^{+}⊂**2**, 4.90 ppm, 6[ZC]) and uncomplexed species (EE-**4**H^{+}, 6[EU]; ZZ-**4**H^{+}, 6[ZU]). On the contrary, photoisomerization does not affect the resonances of methylene protons 1[EC] and 1[ZC] (Figure 4c). Taken together, these results indicate that the presence of ring **2** around the ammonium station has no influence on the photoisomerization process.

Interestingly, the presence of EZ-**4**H^{+} axle – either free or complexed by **2** – could not be observed because diagnostic signals for these species could not be identified in the ^{1}H NMR

spectra. It cannot be excluded that resonances of the *EZ* species overlap with those of the *EE* and/or *ZZ* ones. Nonetheless, their concentration was estimated to be ≤2%.

The association of *ZZ*-**4**H$^+$ with the macrocycle **2**, however, could not be investigated using the same approach adopted for the *EE*-axle. In fact, no complex formation was detected upon mixing equimolar amounts of *ZZ*-**4**H$^+$ (obtained by exhaustive irradiation of the *EE* isomer) and ring **2** within a timeframe where the *E* isomers concentration is constantly ≤5%. This observation is in line with previous studies indicating that when the terminal azobenzene units of the axle are in the *Z* configuration, the kinetic barrier for ring slippage increases dramatically, making these processes very slow at room temperature.[26,27]

To gain more detailed information on the kinetics of complex formation, the equilibrium between axle **4**H$^+$ and **2** was investigated in the dark (*EE*-**4**H$^+$) and upon irradiation (*ZZ*-**4**H$^+$) by means of bidimensional NMR exchange spectroscopy (EXSY, Figure 4). In such experiments, cross peaks are observed for spins that are in slow chemical exchange on the NMR timescale.[29,30] Practically, EXSY spectra were acquired on equimolar solutions of *EE*-**4**H$^+$ and crown ether **2**. The presence of in-phase cross-peaks between the methylene protons of the free *EE*-axle and the *EE*-complex is indicative of chemical exchange (Figure 5a). The magnetization rate constants were extracted, from which the rate constants for threading (k_{in} = 13.2 M^{-1} s^{-1}) and unthreading (k_{out} = 0.049 s^{-1}) were derived (Table 1, see the SI for details).[29,30] These values are quite similar to those previously determined for the system consisting of *EE*-**3**H$^+$ and **2**.[26]

Table 1. Summary of thermodynamic and kinetic constants of the complexation of axles **3**H$^+$ and **4**H$^+$ with ring **2**.[a]

Axle	K [b]	k_{in} [c]	k_{out} [d]
	[L mol^{-1}]	[L mol^{-1} s^{-1}]	[s^{-1}]
EE-**3**H$^+$	820 [e]	24.0	0.029
ZZ-**3**H$^+$	400 [e]	2.9×10^{-3} [e]	7.2×10^{-6} [e]
EE-**4**H$^+$	330	13.2	0.049
ZZ-**4**H$^+$	370[f]	2.1×10^{-3}	5.8×10^{-6}

[a] Uncertainties for all data are reported in the SI. [b] Stability constant of the complex. [c] Threading rate constant. [d] Unthreading rate constant. [e] Data from ref. 26. [f] The stability constant of the complex between *ZZ*-**4**H$^+$ and **2** was estimated from the ratio k_{in}/k_{out}.

Upon exhaustive irradiation at 365 nm of the same solution, nearly all the azobenzene units were converted to the *Z*-form. An EXSY experiment was then carried out under the same conditions (Figure 5b). In this case, however, no in-phase cross peaks between axle *ZZ*-**4**H$^+$ and complex *ZZ*-**4**H$^+$⊂**2** were observed, confirming that the threading and unthreading processes of the *ZZ*-axle are remarkably slower than for the *EE* isomer (Figure 5b).
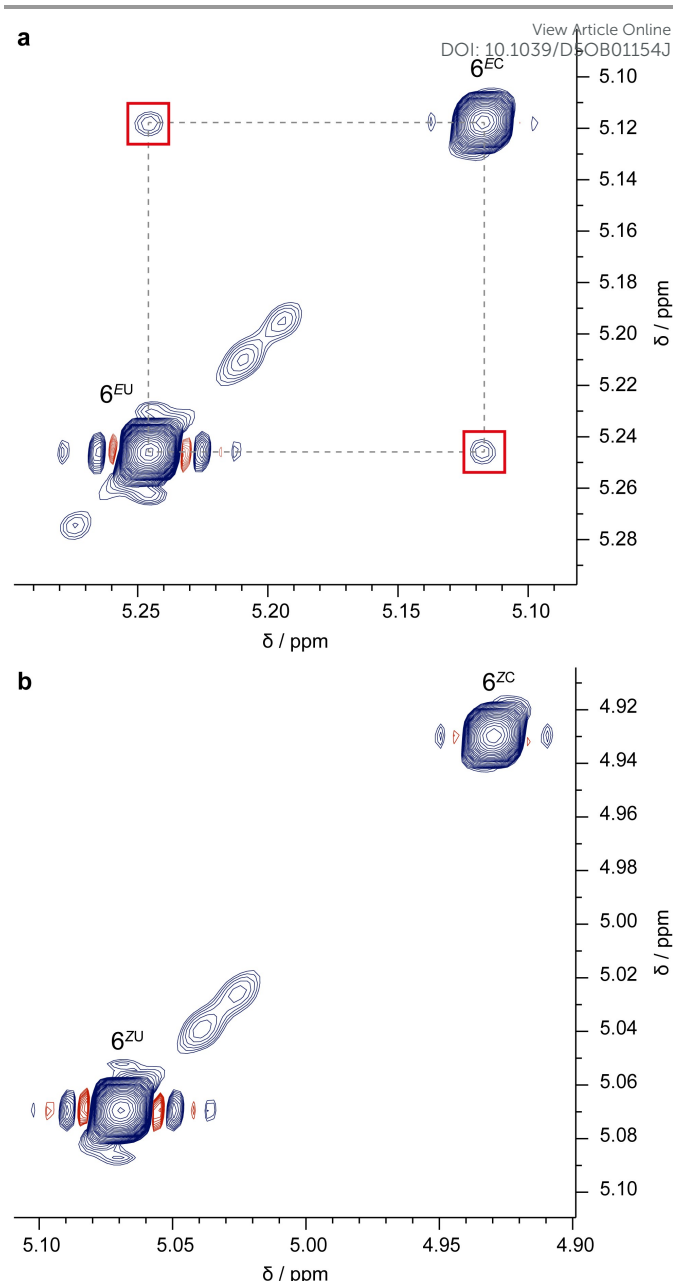

Figure 5. Partial EXSY NMR (CD$_3$CN, 500 MHz, 298 K, 1.4 mM, t_{mix} = 600 ms) spectra of (a) an equimolar mixture of *EE*-**4**H$^+$ and **2**, and (b) the same sample after exhaustive irradiation at 365 nm. 6^{EU} and 6^{EC} in (a) indicates the free and complexed *EE*-axle, respectively, whereas 6^{ZU} and 6^{ZC} in (b) denote the free and complexed *ZZ*-axle, respectively.

The threading and unthreading rate constants of *EE*-**3**H$^+$ reported in ref. 26 were measured with different techniques than those used in the present study. Therefore, the values were redetermined to be consistently compared with *EE*-**4**H$^+$ using 2D EXSY NMR experiments. The results are consistent with those previously obtained (k_{in} = 24 M^{-1} s^{-1} and k_{out} = 0.029 s^{-1}, Table 1 and SI). Subsequently, the sample was irradiated at 365 nm, generating *ZZ*-**3**H$^+$ and *ZZ*-**3**H$^+$⊂**2**, and again submitted to EXSY measurements. Similarly to what was previously observed for *ZZ*-**4**H$^+$⊂**2**, also in this case no chemical exchange

between free and complexed axle could be detected (see the SI).

The formation kinetics of ZZ-**4**H$^+$⊂**2** was therefore investigated by monitoring the time-dependent concentration change of the species upon rapid mixing of ZZ-**4**H$^+$ (obtained by exhaustive irradiation of the EE isomer)‡ and a 10-fold excess of **2** by means of time-resolved ^{1}H NMR spectroscopy. The excess of macrocycle enabled an appreciable complexation of the ZZ-axle within a few hours. The presence of distinct diagnostic resonances (see Figure 4 and the SI) enabled the concentration profiles of the free and complexed axles in their EE and ZZ configurations to be determined. An increase in the population of ZZ-**4**H$^+$⊂**2** (red dots) and the concurrent depletion of the free axle (blue triangles) was observed (Figure 6). The presence of a large excess of macrocycle keeps the concentration of free EE-**4**H$^+$ (black triangles) very low throughout the whole experiment, because nearly all the EE-axle is complexed by **2** (green dots, Figure 6).

The analysis of the time-dependent concentration profiles was carried out in a time window in which the thermal $Z{\rightarrow}E$ back isomerization is negligible, but long enough to observe the formation kinetics of ZZ-**4**H$^+$⊂**2** (up to 50% of its final concentration). Fitting of the time-dependent traces with a mixed order kinetic model allowed us to extract the threading and unthreading rate constants for the ZZ-**4**H$^+$⊂**2** complex (Table 1).
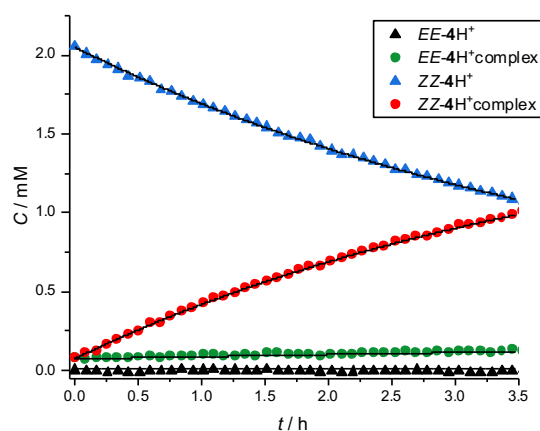

Figure 6. Time-dependent concentration profiles of ZZ-**4**H$^+$⊂**2** (red dots), ZZ-**4**H$^+$ (blue triangles), EE-**4**H$^+$⊂**2** (green dots) and EE-**4**H$^+$ (black triangles). The black lines represent the fitting of the traces. The total concentrations of the axle and the macrocycle, determined from the ^{1}H NMR spectra (CD$_3$CN, 500 MHz, 298 K) are 2.2 mM and 24 mM, respectively.

To gain corroboration of the value of the unthreading rate constant obtained from the fitting of the concentration-time profiles, we performed a ring extrusion experiment using K$^+$ as a competitive guest for **2**. Macrocycle extrusion experiments were performed by adding solid potassium hexafluorophosphate to an acetonitrile solution of the ZZ complex and monitoring its subsequent time-dependent disassembly. KPF$_6$ was selected because: (i) potassium cations form a stable complex with crown ether **2** in acetonitrile (the

stability constant is $7.6{\times}10^3$ M^{-1}, that is, higher than that of both the EE and ZZ complexes)[31]; (ii) both its ions do not significantly affect the ring-axle interaction,[26] and; (iii) KPF$_6$ is silent in the ^{1}H NMR spectra. With these premises, it is expected that K$^+$ displaces ZZ-**4**H$^+$ from **2** and the process is observable by NMR spectroscopy. Practically, a solution containing equimolar amounts of axle EE-**4**H$^+$ (1.6 mM) and ring **2** was exhaustively irradiated at 365 nm to generate the Z species; KPF$_6$ (2.6 equiv, 4.2 mM) was then added and ^{1}H NMR spectra were acquired over time (see the SI). The changes in the resonances of **2** clearly indicate the formation of K$^+$⊂**2** at the expense (unthreading) of ZZ-**4**H$^+$⊂**2**. Fitting of the time-dependent data according to a mixed-order kinetic model yielded the threading ($k_{in} = 4.5{\times}10^{-3}$ M^{-1} s^{-1}) and unthreading ($k_{out} = 4.7{\times}10^{-6}$ s^{-1}) rate constants of ZZ-**4**H$^+$ with **2**. These values are in line with those measured in the absence of K$^+$ cations (Table 1) and confirm the hindering effect of the Z-azobenzene terminal unit on complexation and decomplexation.

Overall, the presence of Z-azobenzene moieties at the extremities of the axle lowers the (un)threading rate constants of more than three orders of magnitude compared to the E-isomer. This observation is in line with the behaviour of the parent axle EE-**3**H$^+$.[26] The stability constant of ZZ-**4**H$^+$⊂**2**, calculated as the ratio between the threading and unthreading rate constants, resulted to be identical (within error) to that of EE-**4**H$^+$⊂**2** (Table 1). Such a result marks a substantial difference of axle **4**H$^+$ with respect to the previously investigated **3**H$^+$, which exhibited an appreciable change in the stability constant on going from the EE to the ZZ isomer. The latter observation could be assigned to the presence of stabilizing π-stacking interactions between the aromatic units of the crown ether and E-azobenzene.[15] While for axle **3**H$^+$ the aromatic azobenzene protons located next to the ammonium (7^{EC}, 3^{EC}, see SI for the full assignment) are markedly shifted upfield upon complexation with **2**, due to π-π stacking interactions with the ring, in axle **4**H$^+$ the same shift is not observed for the photoactive unit. It can be hypothesized that such interactions are weaker in EE-**4**H$^+$ because the azobenzenes, being farther from the recognition site, may not be able to interact with the macrocycle.

On the other hand, the differences observed in the threading and unthreading rate constants with **2**, that are respectively about 5 and 2.5 times slower for EE-**4**H$^+$ than for EE-**3**H$^+$ (Table 1), could be ascribed to the different stiffness of the two axles. While EE-**3**H$^+$ is remarkably rigid and preorganized to threading, EE-**4**H$^+$ has a larger conformational freedom arising from the flexible ethereal linker.[32,33]

Finally, we investigated the possibility to chemically induce unthreading by adding a base capable of deprotonating the ammonium centre of the axle.[24,26,34,35] Deprotonation of the axle yields a neutral amine that, according to earlier investigations,[34,36] should exhibit a negligible affinity for the crown ether. Unfortunately, treatment of axle EE-**4**H$^+$ (both free and complexed by **2**) with either triethylamine or a resin-bound amine resulted in the formation of a precipitate which prevented further investigations (see the SI).

ARTICLE

Conclusion

A novel symmetrical azobenzene-dibenzylammonium axle was prepared, and the thermodynamic and kinetic properties of its pseudorotaxane complex with dibenzo-24-crown-8 were investigated both in the dark and upon light irradiation. The axle differs from a previously investigated one[26,27] in which the azobenzene units are closer to the secondary ammonium center and share a phenyl ring with it. In the present compound the photoactive and recognition moieties are spatially and electronically decoupled. Such a strategy allowed to study how the *E/Z* configuration of the azobenzene groups affects the stability of the pseudorotaxane and its threading-unthreading rates. Furthermore, the separation allowed us to qualitatively understand how these two aspects are related – an information which is important to develop light-driven molecular pumps with non-symmetrical axles based on similar designs.[15,24] Our results confirm that *Z*-azobenzene slows down the threading-unthreading into/from the macrocycle much more efficiently than the *E*-isomer, which is a crucial requirement for implementing a light-triggered energy ratchet mechanism. However, the stability of the complex is unaffected by the configuration of the azobenzene extremities of **4**H^{+}; this observation highlights the significance of the other basic requirement of energy ratchet, namely the destabilization of the complex caused by light, which provides the driving force for unthreading.

This study, on the one hand, confirms the modular nature of this kind of systems, in which the azobenzene and secondary ammonium units of the axle perform specific and distinct roles in the self-assembly with the macrocycle. On the other hand, the present investigation highlights the importance of the close proximity of such units to simultaneously affect the thermodynamic stability and the kinetic lability of the pseudorotaxane. Our data indicate that these properties are not solely governed by steric factors: intermolecular electronic interactions, such as π-stacking, most likely play a major role.

Author contributions

Conceptualization: A.C. and M.B.; methodology: M.B. and S.C.; experimental investigations: B.S. and C.T.; data analysis: B.S., C.T., S.C. and M.B.; funding acquisition: A.C.; writing-original draft: S.C. and A.C.; writing-review and editing: all authors. All authors participated to discussions, edited the manuscript and approved its final form.

Conflicts of interest

There are no conflicts to declare.

Data availability

The data supporting this article have been included as part of the Supplementary Information.

Acknowledgements

Notes and references

‡ The *E→Z* conversion was >98%; as our data indicate that the two azobenzene units behave independently from one another, the statistical distribution of the species would be >97% *ZZ*-**4**H^{+}; <2% *EZ*-**4**H^{+}; <1% *EE*-**4**H^{+}.

1   S. Kassem, T. van Leeuwen, A. S. Lubbe, M. R. Wilson, B. L. Feringa and D. A. Leigh, Artificial molecular motors. *Chem. Soc. Rev.*, 2017, **46**, 2592-2621.

2   C. Pezzato, C. Cheng, J. F. Stoddart, and R. D. Astumian, Mastering the non-equilibrium assembly and operation of molecular machines. *Chem. Soc. Rev.*, 2017, **46**, 5491-5507.

3   M. Baroncini, L. Casimiro, C. De Vet, J. Groppi, S. Silvi and A. Credi, Making and operating molecular machines: a multidisciplinary challenge. *ChemistryOpen*, 2018, **120**, 200-268.

4   F. Lancia, A. Ryabchun and N. Katsonis, Life-like motion driven by artificial molecular machines. *Nat. Rev. Chem.,* 2019, **3**, 536-551.

5   A. Perrot, E. Moulin and N. Giuseppone, Extraction of mechanical work from stimuli- responsive molecular systems and materials. *Trends Chem.*, 2021, **3**, 926-942.

6   Y. Qiu, Y. Feng, Q. H. Guo, R. D. Astumian and J. F. Stoddart, Pumps through the ages. *Chem*, 2020, **6**, 1952-1977.

7   Y. Feng, M. Ovalle, J. S. W. Seale, C. K. Lee, D. J. Kim, R. D. Astumian and J. F. Stoddart, Molecular pumps and motors. *J. Am. Chem. Soc.*, 2021, **143**, 5569-5591.

8   L. Zhang, H. Wu, X. Li, H. Chen, R. D. Astumian, J. F. Stoddart, Artificial molecular pumps. *Nat. Rev. Met. Prim.*, 2024, **4**, 13.

9   D. S. Goodsell, *The machinery of life. Second edition*. Copernicus, New York, 2009.

10 C. Cheng, P. R. McGonigal, S. T. Schneebeli, H. Li, N. A. Vermeulen, C. Ke and J. F. Stoddart, An artificial molecular pump. *Nat. Nanotechnol.*, 2015, **10**, 547-553.

11 S. Amano, S. D. P. Fielden and D. A. Leigh, A catalysis-driven artificial molecular pump. *Nature*, 2021, **594**, 529-534.

12 L. Binks, C. Tian, S. D. P. Fielden, I. J. Vitorica-Yrezabal, D. A. Leigh, Transamidation-driven molecular pumps. *J. Am. Chem. Soc.*, 2022, **144**, 15838-15844.

13 C. K. Lee, J. P. Violi, W. A. Donald, J. F. Stoddart, D. J. Kim, Controlled assembly of rotaxane translational isomers using dual molecular pumps. *Nat. Commun.*, 2025, **16**, 5922.

14 C. Pezzato, M. T. Nguyen, D. J. Kim, O. Anamimoghadam, L. Mosca and J. F. Stoddart, Controlling dual molecular pumps electrochemically. *Angew. Chem. Int. Ed.*, 2018, **57**, 9325-9329.

15 G. Ragazzon, M. Baroncini, S. Silvi, M. Venturi and A. Credi, Light-powered autonomous and directional molecular motion of a dissipative self-assembling system. *Nat. Nanotechnol.*, 2015, **10**, 70-75.

16 S. Corra, L. Casimiro, M. Baroncini, J. Groppi, M. La Rosa, M. Tranfić Bakić, S. Silvi and A. Credi, Artificial supramolecular pumps powered by light. *Chem. Eur. J.*, 2021, **27**, 11076-11083.

17 M. Canton, J. Groppi, L. Casimiro, S. Corra, M. Baroncini, S. Silvi and A. Credi, Second-generation light-fueled supramolecular pump. *J. Am. Chem. Soc.*, 2021, **143**, 10890-10894.

18 T. Sangchai, S. Al Shehimy, E. Penocchio and G. Ragazzon, Artificial molecular ratchets: tools enabling endergonic processes. *Angew. Chem. Int. Ed.* 2023, **62**, e202309501.

19 S. Borsley, D. A. Leigh and B. M. W. Roberts, Molecular ratchets and kinetic asymmetry: giving chemistry direction. *Angew. Chem. Int. Ed.*, 2024, **63**, e202400495.

20 M. Kathan and S. Hecht, Photoswitchable molecules as key ingredients to drive systems away from the global thermodynamic minimum. *Chem. Soc. Rev.*, 2017, **46**, 5536-5550.

21 M. Weissenfels, J. Gemen and R. Klajn, Dissipative self-assembly: fueling with chemicals versus light. *Chem*, 2021, **7**, 23-37.

22 S. Corra, M. Curcio and A. Credi, Photoactivated artificial molecular motors. *JACS Au*, 2023, **3**, 1301-1313.

23 S. Corra, M. Tranfic Bakić, J. Groppi, M. Baroncini, S. Silvi, E. Penocchio, M. Esposito and A. Credi, A Kinetic and energetic insights into the dissipative non-equilibrium operation of an autonomous light-powered supramolecular pump. *Nat. Nanotechnol.*, 2022, **17**, 746-751.

24 M. Baroncini, S. Silvi, M. Venturi and A. Credi, Photoactivated directionally controlled transit of a non-symmetric molecular axle through a macrocycle. *Angew. Chem. Int. Ed.*, 2012, **51**, 4223-4226.

25 A. Li, Y. Tang, Z. Du, X. Wang, Q. Yang, Y. Wu, X. Li, K. Zhu, Accelerating or slowing: fine tuning the de-threading kinetics of a T-shaped benzimidazolium pumping cassette. *Chem. Eur. J.*, 2025, **31**, e202501605.

26 M. Baroncini, S. Silvi, M. Venturi and A. Credi, Reversible photoswitching of rotaxane character and interplay of thermodynamic stability and kinetic lability in a self-assembling ring-axle molecular system. *Chem. Eur. J.*, 2010, **16**, 11580-11587.

27 G. Tabacchi, S. Silvi, M. Venturi, A. Credi and E. Fois, Dethreading of a photoactive azobenzene-containing molecular axle from a crown ether ring: a computational investigation. *ChemPhysChem*, 2016, **6**, 1913-1919.

28 P. R. Ashton, M. C. T. Fyfe, S. K. Hickingbottom, J. F. Stoddart, A. J. P. White and D. J. Williams, Hammett correlations "beyond the molecule". *J. Chem. Soc. Perkin Trans. 2*, 1998, 2117-2128.

29 J. Lu, J. Hu, W. Tang, and D. Zhu, Nuclear magnetic resonance spectroscopic studies of pyridine methyl derivatives binding to cytochrome C. *J. Chem. Soc. Dalton Trans.*, 1998, 2267-2274.

30 Z. Zolnai, N. Juranić, D. Vikić-Topić and S. Macura, Quantitative determination of magnetization exchange rate constants from a series of two-dimensional exchange NMR spectra. *J. Chem. Inf. Comput. Sci.*, 2000, **40**, 611-621.

31 Y. Takeda, Y. Kudo and S. Fujiwara, Thermodynamic study for complexation reactions of dibenzo-24-crown-8 with alkali metal ions in acetonitrile. *Bull. Chem. Soc. Jpn.* 1985, **58**, 1315-1316.

32 J. Cao, M. C. T. Fyfe, and J. F. Stoddart, Molecular Shuttles by the Protecting Group Approach. *J. Org. Chem.* 2000, **65**, 1937-1946.

33 P. G. Young, K. Hirose, and Y. Tobe, Axle Length Does Not Affect Switching Dynamics in Degenerate Molecular Shuttles with Rigid Spacers. *J. Am. Chem. Soc.* 2014, **136**, 7899-7906.

34 A. Credi, M. Montalti, V. Balzani, S. J. Langford, F. M. Raymo and J. F. Stoddart, Simple molecular-level machines. Interchange between different threads in pseudorotaxanes. *New J. Chem.*, 1998, **22**, 1061-1065.

35 M.-L. Yen, W.-S. Li, C.-C. Lai, I. Chao and H. S. Chiu, Dual-action acid/base- and base/acid-controllable molecular switch. *Org. Lett.*, 2006, **8**, 3223-3226.

36 P. R. Ashton, R. Ballardini, V. Balzani, M. Gomez-Lopez, S. E. Lawrence, M. V. Martinez-Diaz, M. Montalti, A. Piersanti, L. Prodi, J. F. Stoddart and D. J. Williams, Molecular meccano. 26. Hydrogen-bonded complexes of aromatic crown ethers with (9-anthracenyl)methylammonium derivatives. Supramolecular photochemistry and photophysics. pH-controllable supramolecular switching. *J. Am. Chem. Soc.*, 1997, **119**, 10641-10651.

Organic & Biomolecular Chemistry Accepted Manuscript

Light-driven molecular pumps. Understanding the entanglement of thermodynamic and kinetic effects in the photo-controlled threading-unthreading of azobenzene-ammonium pseudorotaxanes

Brian Sachini, [a, b] Chiara Taticchi, [a, b] Massimo Baroncini, [b, c] Stefano Corra, [a,b] and Alberto Credi, *[a,b]

[a.] *Dipartimento di Chimica Industriale "Toso Montanari", Alma Mater Studiorum - Università di Bologna, Via Gobetti 85, 40136, Bologna, Italy.*

[b.] *Center for Light Activated Nanostructures (CLAN), Istituto ISOF-CNR, via Gobetti 101, 40129 Bologna, Italy.*

[c.] *Dipartimento di Scienze e Tecnologie Agro-Alimentari, Alma Mater Studiorum - Università di Bologna, Viale Fanin, 40-50, 40127, Bologna, Italy.*

Data Availability Statement

The data supporting this article have been included as part of the Supplementary Information.